2013 ISES Solar World Congress

Spatial and temporal variability of PV output in an insular grid: Case of Reunion Island

Mathieu David[a*], Faly H. Ramahatana Andriamasomanana[a], Olivier Liandrat[b]

aPIMENT, University of La Reunion, 117 rue du Geneal Ailleret, 97430 Tampon, Reunion Island
bReuniwatt, 14 rue de la Guadeloupe, 97490 Saint-Clotilde, Reunion Island

Abstract

Some small territories, such islands, actually experience a high penetration rate of PV inside a small electricity grid. In this context, the variability of the PV output is an issue for the supply-demand balance. The spatial and temporal smoothing of the variability of the PV production is an important information for the grid operator.
Previous works on this topic were mainly done for large-scale continental grids. They pointed out the relation between the production variability with the number and the dispersion factor of the PV systems. This paper presents an analysis of the variability of PV output for a small insular territory: Reunion island. This island has a large variety of microclimates and a strong penetration rate of PV (almost 30% of the installed power). For this little grid, the spatial and temporal effects on the variability of the PV output differ slightly with previous works.

1. Introduction

Between 2005 and 2011, the French government set up an incentive policy in order to develop the electricity production from photovoltaic. In the overseas territories, as Reunion Island, the feed-in tariffs proposed for the next 20 years were specifically high [1]. It results an exponential increase of the installed PV systems (Fig. 1). For these small grids, an important penetration rate of such a variable means of production can destabilize the supply-demand balance. A regulatory limit of 30% of the instantaneous power produced from intermittent renewables (PV, wind turbines) was defined in order to avoid this risk. This legal constraint was reached in 2012 in Reunion. In this context, the knowledge of spatial and temporal short-term variability of the PV output power is essential. In one hand, it will help the grid

* Corresponding author. Tel.: +262-262-579-249
E-mail address: mathieu.david@univ-reunion.fr

operator to better manage the different means of production. Second, it will permit to stretch the mandatory limit of 30% and so to increase the penetration rate of PV.

The short-term variability of the solar resource is generated by variable cloudiness conditions. The considered time scales range from few seconds to one hour. The solar fluctuations on short time scales were firstly studied in terms of frequency distribution of the instantaneous clearness index [2][3][4][5]. More recently, numerous articles dealing with the PV output power variability propose new indices in order to quantify the temporal fluctuations of the solar resource. Lave and Kleissl [6][7] used the statistical distributions of the Ramp Rates (RRs). RRs relate to the sudden changes in power output or in solar irradiance. Hoff and Perez introduced the standard deviation of the change in power output to quantify the short-term variability [8][9][10]. These works were mainly focus on continental territories. This work will focus on this second approach in order to assess the temporal and spatial variability of the PV production.

Reunion Island exhibits a particular meteorological context dominated by a large diversity of microclimates. Two main regimes of cloudiness are superposed: the clouds drived by the synoptic conditions over the Indian Ocean and the orographic cloud layer generated by the local reliefs. Badosa et al. did a first study about the solar variability in Reunion [11]. They characterized the daily fluctuations using hourly profiles of irradiance of 7 ground stations. Identical weather conditions can be encountered in Hawaii. Hoff and Perez included this island in their study about the correlation of the solar variability between different sites [11]. They used the same method for Hawaii and for the continental territories of the US.

In this work, the spatial and temporal variability will be studied and compared with the results of previous works on the topic.

2. Methodology

This section describes the methods and indices used in order to quantify the variability of the PV power output. This variability is directly linked with the variability of the solar resource. Thus, the proposed methods and indices are mainly derived from the ground measurements or assessment from satellite images of the solar irradiance.
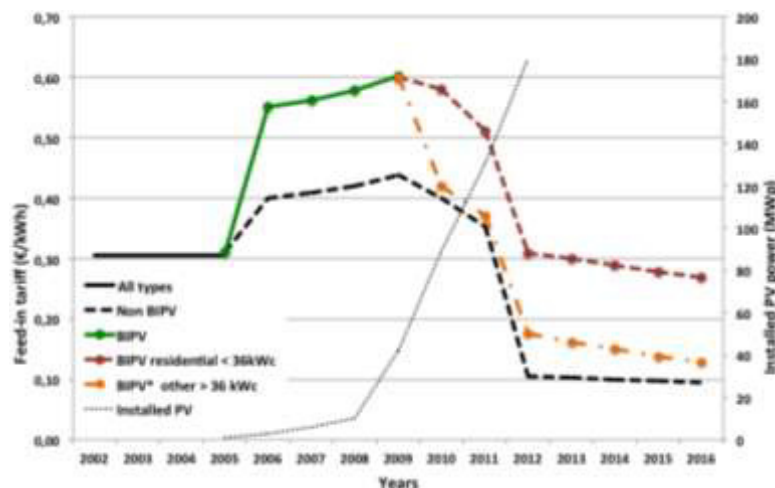

Fig. 1. Evolution of the feed-in tariffs [1] and installed PV power in Reunion

2.1. Temporal variability

The variability of a single PV system is quantified by the standard deviation $\sigma_{\Delta t}$ of the change in power output $\Delta P_{\Delta t}$ for a considered time interval Δt [10].

$$\sigma_{\Delta t} = \sqrt{Var(\Delta P_{\Delta t})} \tag{1}$$

For a PV fleet, the variability is evaluated considering the aggregate power output and it can be derived from the variability of each single system. In order to quantify the PV fleet variability, Hoff and Perez [11] proposed two models. In the first model, they consider that the changes in the output of the plants are uncorrelated. It has been shown previously that the changes in solar irradiance between two locations can be partially correlated [9][12]. So, they established a more realistic model for correlated locations. We will focus on this second model given in Eq. (2) that requires the knowledge of each plant variability and the correlations between the different locations $\rho_{\Delta t}^{i,j}$.

$$\sigma_{\Delta t}^{fleet} = \sqrt{\sum_{i=2}^{N} \sum_{j=1}^{i} \sigma_{\Delta t}^{i} \cdot \sigma_{\Delta t}^{j} \cdot \rho_{\Delta t}^{i,j}} \tag{2}$$

The temporal short-term variability of the PV output power is directly linked with the fluctuation of the global horizontal irradiance *GHI*. In order to take only into account the effects of these fluctuations, it is important to remove the seasonal variation of the solar radiation. This deterministic part is commonly modeled by the global irradiance observed for a clear sky *GHI*_{clear}. The clear sky index *Kt** as defined in Eq. 3 was created for this purpose.

$$Kt^* = \frac{GHI}{GHI_{clear}} \tag{3}$$

Finally, the variability of the solar resource for a site can be assessed using the changes in clear sky index for a considered time interval $\Delta Kt_{\Delta t}^*$.

2.2. Cloud speed

It has been shown that the cloud speed affects significantly the solar variability for a site and also the correlation between sites [8]. Several methods were developed to derive the cloud speed. Hoff and Perez assess a relative cloud speed using satellite images [10]. Their method is based on the concept of cloud motion vectors initially developed for forecasting. Two recent articles propose some methods in order to derive the cloud speed from ground measurements [13][14]. These methods need a large number of sensors or cameras and are not suitable in order to cover a large area. Finally, Lave and Kleissl use the NOAA North American Mesoscale (NAM) numerical weather forecast [15]. They assessed the height of the cloud layers with the vertical profile of the relative humidity. In this work, we used a similar method with the help of the Global Forecast System (GFS) model. The spatial resolution is 0.5° (55km x 55km) and the temporal resolution is 3 hours. A linear interpolation of the weather parameters was done in order to fit with the considered time scale. The main cloud layer is supposed to be situated at an altitude where the relative humidity is the highest (Fig. 2). The wind speed and direction at this altitude are used as an approximation of the cloud motion. If the vertical profile of the relative humidity is never higher than 90%, a clear sky is considered.
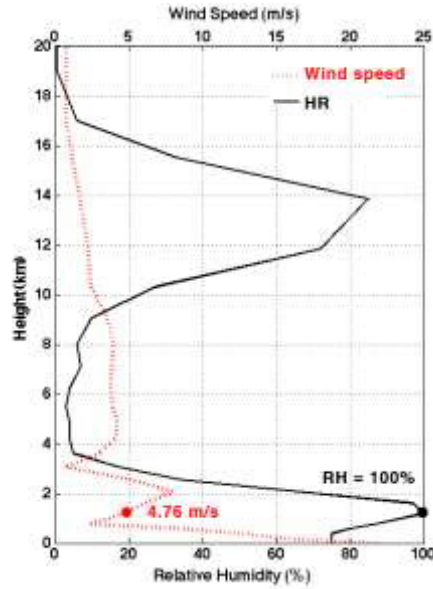
Fig. 2. Plot of the profile of relative humidity and wind speed on January 1st 2011 at Reunion. In this example, the main cloud layer was found to be at about 1200m, with a speed of 4.76 m/s.

2.3. Pair sites correlation

As presented in the sub-section 2.1, the temporal variability of a fleet of PV systems is dependent on the correlation of the variability between the different locations. The correlation coefficient (Pearson's formula) of changes in clear-sky index is defined in Eq. 4. This pair site correlation coefficient is highly dependent on the distance between sites, the time scale and the cloud speed [10].

$$\rho^{i,j} = \frac{cov\left[\Delta Kt^{*i}_{\Delta t}, \Delta Kt^{*j}_{\Delta t}\right]}{\sigma_i \times \sigma_j} \tag{4}$$
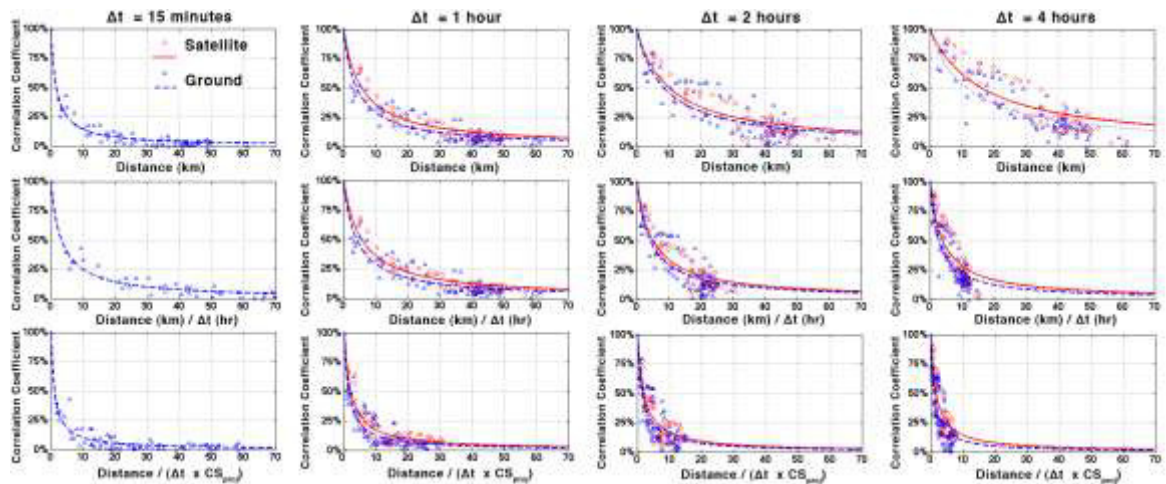

Fig. 3. Pair site correlation coefficients presented by time interval as a function of distance, time scale and projected cloud speed.
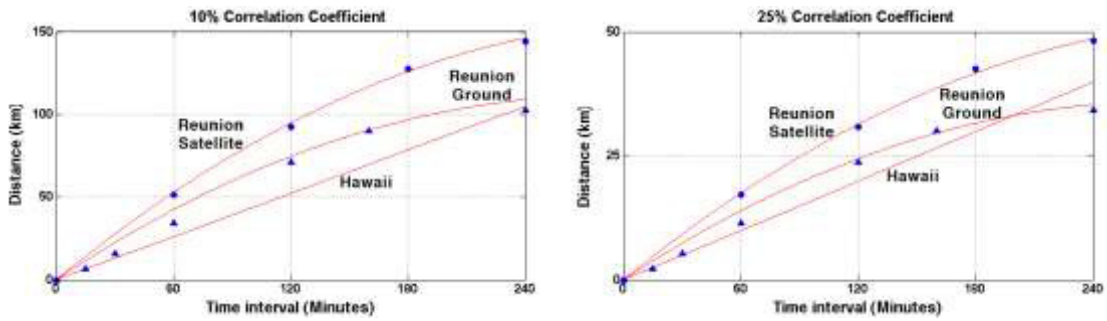
Fig. 4. Mean distance for a fixed correlation coefficient as a function of the time interval for Reunion (ground and satellite) and for Hawaii [10].

2.4. Spatial variability

Perez et al. proposed a metric in order to quantify the spatial variability [16]. It corresponds to the standard deviation of the satellite derived clear-sky index σ_{space} of the pixel surrounding the considered location as given in Eq. 5. In this formula, N is an odd number greater or equal to 3, Kt^* is the satellite derived clear-sky index and $\overline{Kt^*}$ is the mean index across the extended area. For this analysis, the number of considered pixels N^2 is equal to 9 and hourly satellite data are used. In order to differentiate the high and low spatial variability, a threshold of 0.1 was defined [16].

$$\sigma_{space} = \frac{1}{N} \sqrt{\sum_{i=1}^{N^2} (Kt^{*i} - \overline{Kt^*})^2} \qquad (5)$$
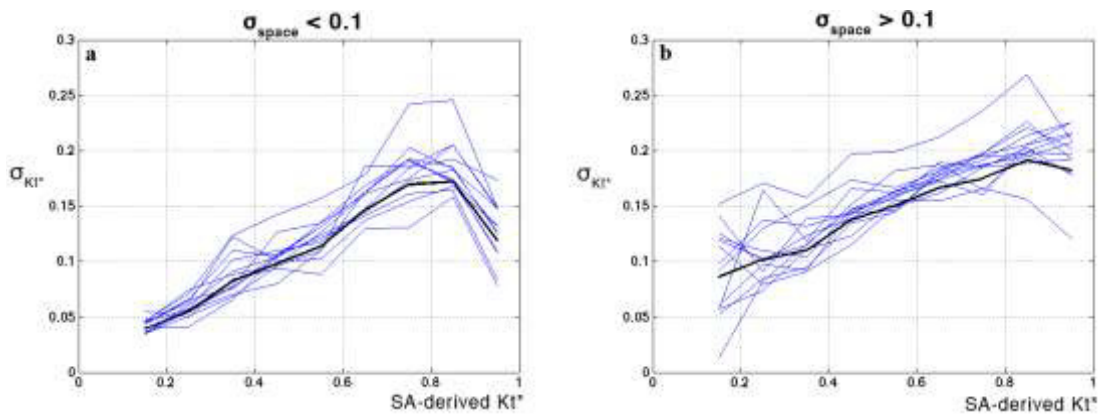

Fig. 5. One-minute σ_{Kt^*} metric trends as a function of satellite derived Kt^* for low spatial variability (a) and high spatial variability (b). Each blue line represents an individual site. The bold black line represents the mean trend derived for all sites.
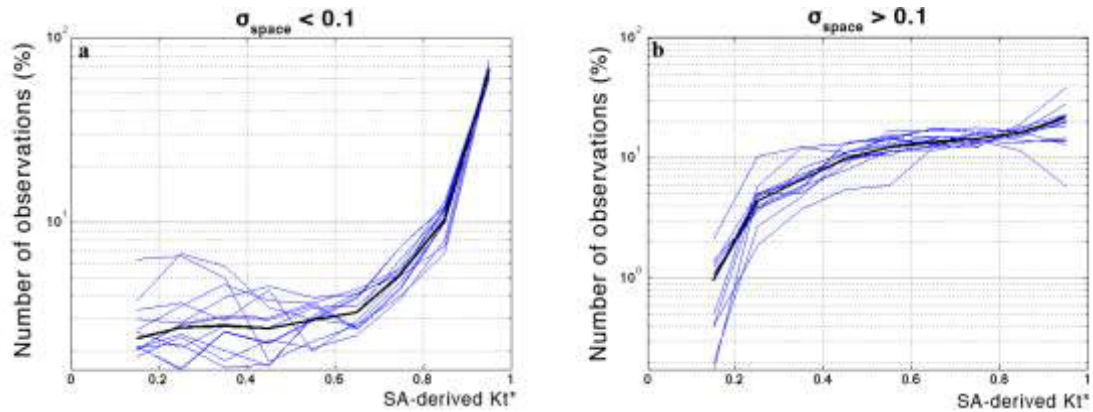
Fig. 6. Number of minute observations as a function of satellite derived Kt^* for low spatial variability (a) and high spatial variability (b). Each blue line represents an individual site. The bold black line represents the mean trend derived for all sites.

3. Results and discussion

3.1. Data

13 locations distributed in the main PV areas of Reunion were considered for this work. For each of these sites, one-minute ground measurements of the GHI were provided by the company Reuniwatt (11 sites) and the PIMENT laboratory (2 sites). The data of Reuniwatt and PIMENT were recorded respectively since 2010 and 2006. The satellite derived GHI and clear-sky indices were provided by the ASRC, State University of New York at Albany. The size of the pixels is 0.05°x0.05° (5.5 km). They cover a square of 1.6° (approximately 178 km) of latitude and longitude including Reunion Island and surrounding sea. The time step is one hour and the satellite images were observed during 5 years between 2008 and 2012.

3.2. Influence of the time scale and cloud speed on the pair site correlation coefficient

The site pair correlation coefficient decreases with increase of the distance between two sites d^{ij} for both satellite and ground observations. The relationship can be assessed with the formula given in Eq. 6 and is represented by the continuous line in Fig. 3 [10][11]. The parameter D is called the "decorrelation" distance and it corresponds to the distance where the correlation coefficient is equal to 0.5. The decorrelation distance is lower for the satellite images because of the spatial smoothing.

$$\rho^{i,j} = \frac{1}{1 + d^{ij}/D} \qquad (6)$$

The time scale of the data influences significantly the value of the decorrelation distance. Hoff and Perez assume a linear relationship between the time scale and the parameter D [10]. The results obtained with the ground data measurements of Reunion are closed to the linear regression of Hawaii (Fig. 4). A better fitting curve can be achieved using a polynomial function. In Fig. 10, a quadratic function was used for the ground and satellite observation of La Reunion.

The raw cloud speed and direction evaluated with the procedure described in sub-section 2.2 were not used directly. A projection of the motion vector of the clouds C_{motion} was done on the distance separating

the different locations (Eq. 7). At each time step the distance between the sites was divided by the results of the projection and by the time scale.

$$CS_{proj} = \overrightarrow{C_{motion}} \cdot \overrightarrow{d^{ij}} \qquad (7)$$

Adding in Eq. 6 the two parameters relative to the time scale Δt and the projected cloud speed CS_{proj}, the pair site correlation coefficient can be assessed using Eq. 8. Fig. 3 shows the results for the ground data and the satellite images at different time scales.

$$\rho^{i,j} = \frac{1}{1 + d^{ij}\big/_{D \cdot \Delta t \cdot CS_{proj}}} \qquad (8)$$

With at least one year of data, the analysis was done for relatively long time series of solar irradiance. The correlation coefficients are calculated over the whole time period. Thus, the results are representative of the average behavior during the studied period.

3.3. Spatial variability versus temporal variability

Fig. 6 presents the distribution of the ground measurements. For a high spatial variability ($\sigma_{space} > 0.1$), the distribution of the $Kt*$ is almost constant between 0.4 and 1. Contrariwise, for a low spatial variability ($\sigma_{space} < 0.1$), 80% of the observations correspond to clear skies with a $Kt*$ ranging between 0.8 and 1. This second distribution is significantly different from the work of Perez et al. [16] that presents a bimodal shape with a large number of observed overcast skies. The measurements were done in the main PV areas where the solar potential is the most important of the island (>1.8MWh/m^2/year). This is why we mainly observed clear sky conditions.

Fig. 5 presents the trend of the hourly standard deviation of the minute $Kt*$ for each sites as a function of the satellite derived $Kt*$ and for the two conditions of spatial variability. In both cases, temporal variability of the clearness index seems to follow a similar shape for all the sites. As proposed by Perez et al. [16], a robust parameterization of the site-specific short-term variability can be achieved using spatial information.

Satellite data are currently available with a rough time scale of half an hour. The knowledge of the relationship between the spatial variability and the short-term temporal variability is essential. It will permit to assess the level of temporal variability without needs of high frequency ground measurements. This approach is complementary to a spatially distributed method of forecast, like cloud motion vectors approach or numerical weather prediction software.

4. Conclusion

Different metrics and data sources were used in order to characterize the spatial and temporal variability of the solar irradiance. Even if the climatic conditions of Reunion differ highly with the continental sites studied in most other works, the trends are relatively well reproduced. Because of the proximity of very different microclimates, some light differences are observed for the studied metrics. The distance of decorrelation in Reunion is shorter than the continental regions. So, the smoothing effect of the spatial distribution is higher for this small territory. The results of this study improve the knowledge of the relationships between the spatial and temporal variability. They can be applied to the grid management and they can also be used in order to refine the forecast of the PV output power.

Acknowledgements

The authors would like to thank the Reuniwatt society for providing their ground measurements and the SRC, University of Albany, for providing the satellite derived GHI and clear-sky index.

References

[1] Praene JP, David M, Sinama F, Morau D, Marc O. *Renewable energy: Progressing towards a net zero energy island, the case of Reunion Island Review*. Renewable and Sustainable Energy Reviews 2012;16:426-442.

[2] Skartveit A, Olseth JA. *The probability density andautocorrelation of short-term global and beam irradiance*. Solar Energy 1992;249:477–487.

[3] Gansler RA, Klein SA, Beckman WA. *Investigation of minute solar radiation data*. Solar Energy 1995;55:21-27.

[4] Vijayakumar G, Kummert M., Klein SA, Beckman WA. *Analysis of short-term radiation data*. 2005;79:495-504.

[5] Woyte A, Belmans R, Nijs J. *Fluctuations in instantaneous clearness index: Analysis and statistics*. Solar Energy 2007;81:195-206.

[6] Lave M, Kleissl J. *Solar variability of four sites across the state of Colorado*. Renewable Energy 2010;35:2867-2873.

[7] Lave L, Kleissl J, Arias-Castro E. *High-frequency fluctuations and geographic smoothing*. Solar Energy 2012;86:2190-2199.

[8] Hoff TE, Perez R. *Quantifying PV power Output Variability*. Solar Energy 2010;84:1782-1793.

[9] Mills A, Wiser R. *Implication of Wide-Area Geographic Diversity for Short-Term Variability of Solar Power*. Lawrence Berkeley National Laboratory Technical Report LBNL-3884E; 2010

[10] Hoff TE, Perez R. *Modeling PV fleet output variability*. Solar Energy 2012;86:2177-2189.

[11] Badosa J, Haeffelin M, Chepfer H. *Scales of spatial and temporal variation of solar irradiance on Reunion tropical island*. Solar Energy 2013;88:42-56.

[12] Lorenz E, Hurka J, Heinemann D, Beyer HG. *Irradiance forecasting for the prediction of grid-connected photovoltaic systems*. IEEE Journal of selectd topics in appleid earth observations and remote sensing 2009;2:2-10.

[13] Chow CW, Urquhart B, Lave M, Domingez A, Kleissl J, Sheilds J, Washom B. *Intra-hour forecasting with a total sky imager at the UC San Diego solar testbed*. Solar Energy 2011;85:2881-2893.

[14] Bosch JL, Zheng Y, Kleissl J. *Deriving cloud velocity from an array of solar radiation measurements*. Solar Energy 2013;87:196-203.

[15] Lave M, Kleissl J. *Cloud speed impact on solar variability scaling – Application to the wavelet variability model*. Solar Energy 2013;91:11-21.

[16] Perez R, Kivalov S, Schlemmer J, Hemker K, Hoff TE. *Short-term irradiance variability: Preliminary estimation of station pair correlation as a function of distance*. Solar Energy 2012;86:2170-2176.